INTERNATIONAL JOURNAL FOR NUMERICAL METHODS IN FLUIDS
Int. J. Numer. Meth. Fluids 2006; **52**:31–61
Published online 10 February 2006 in Wiley InterScience (www.interscience.wiley.com). DOI: 10.1002/fld.1091

Stability of high-speed two-layer film casting of Newtonian fluids

Jing Zhang, Roger E. Khayat*,† and Wei Wang

Department of Mechanical and Materials Engineering, The University of Western Ontario, London, Ont., Canada N6A 5B9

SUMMARY

The steady-state flow and its linear stability are investigated for the isothermal two-layer film casting process. Newtonian fluids are considered in this study. The continuity of traction is ensured at the interface, and the axial velocity is assumed to be uniform across each film layer separately. The effects of inertia, gravity, fluid parameters and processing conditions on the steady-state flow and its stability are studied. The results indicate that the fluid properties and the processing conditions have significant influence on the flow. The flow stability is strongly dependent on the layer layout with respect to the take-up rolling process. The frequency of the (unstable) disturbance is insensitive to flow and processing parameters. Copyright © 2006 John Wiley & Sons, Ltd.

KEY WORDS: two-layer film casting; thin film flow; linear stability

1. INTRODUCTION

In a typical film casting operation, the molten polymer is extruded through a slit die and is taken up by a rotating cold roll, the 'chill' roll, as illustrated in Figure 1. The velocity at the take-up point is much larger than the extrusion velocity at the die. The molten film is normally stretched and drawn to reduce its thickness. The desired film thickness can be obtained by choosing the appropriate draw ratio (ratio of the take-up velocity to the extrusion velocity at the die exit). In industrial practice, the film casting operation is frequently limited at a certain draw ratio by an instability known as draw resonance, which appears at high draw ratios. There exists a critical draw ratio, beyond which stable operation is impossible and draw resonance defect is observed. This defect consists of a periodic variation in the thickness across the entire width of the film. Thus, better understanding of the molten polymer performance in the stretching stage is important. The numerical simulation presented in this paper focuses on the stretching stage.

*Correspondence to: Roger E. Khayat, Department of Mechanical and Materials Engineering, The University of Western Ontario, London, Ont., Canada N6A 5B9.
†E-mail: rkhayat@eng.uwo.ca

Received 6 July 2005
Accepted 22 August 2005

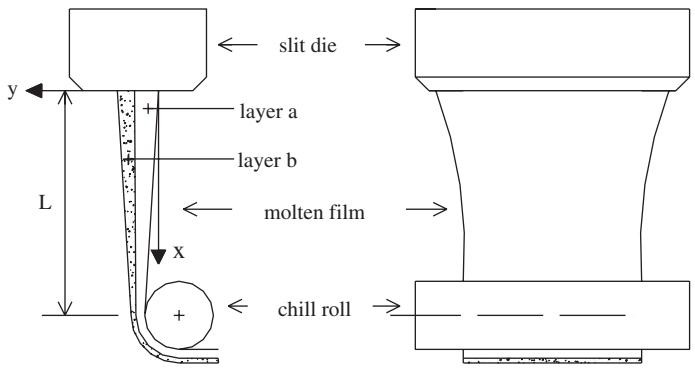

Figure 1. Schematic illustration of the two-layer film casting process.

Although the film casting process is an important industrial operation to manufacture polymeric film, experimental and theoretical studies on the process are limited and most of the previous works focused on single-layer flow. The pioneering work of Yeow [1] examined the Newtonian steady-state solution for the film casting process and its linear stability to three-dimensional infinitesimal flow disturbances. Surface tension was neglected, and so were fluid inertia, gravitational forces, and aerodynamic drag in his study. Also, small film thickness variation and uniform axial stress across the film thickness were assumed. In the linear stability analysis, the linearly independent solutions are obtained by solving the eigenvalue problem as an initial-value problem. The numerical simulation methods involve the standard fourth-order Runge–Kutta procedure. Yeow found that the critical draw ratio for instability to occur was equal to $D_R = 20.21$. However, it is well known that commercial film casting can be operated at a draw ratio larger than 20.21 without encountering draw resonance. Several factors contribute to this enhanced stability. One of the factors is the non-Newtonian behaviour of the molten polymer. Extensive work has been done to investigate the non-Newtonian effects [2–6]. Another important factor is inertia effect, which has been neglected in the literature. Inertia becomes significantly important in modern high-speed film casting, and is one of the objects in the present study.

Co *et al.* [2] and Papanastasiou *et al.* [3] examined viscoelastic flow of the film casting process. Co *et al.* conducted a steady-state analysis and a linear stability analysis for three-dimensional disturbances in the flow that obeys a modified convected Maxwell model. In the linear stability analysis, the eigenvalue problem was treated as a two-boundary problem. They found that a lower and an upper critical draw ratio exist for the film casting of the viscoelastic fluid. The flow was stable below a lower critical draw ratio and above an upper critical draw ratio. Their analysis also showed that the non-Newtonian characteristic of shear thinning enlarges the region of instability. Papanastasiou *et al.* studied isothermal and non-isothermal film casting by means of a BKZ-type nonlinear, integral constitutive equation, which accounts for multiple relaxation times, shear-thinning, extension-thinning or thickening and for the shear-prehistory inside the die. The Galerkin finite-element method was employed to solve the governing equations. The unknown variables are approximated by a series expansion by means of known quadratic finite-element basis functions. The resulted system of nonlinear, algebraic equations was solved using full Newton-iteration technique. The numerical results

were compared with the experimental data of the casting of polypropylene. Good agreement was obtained for the film thickness and the temperature profiles. For more general references on single-layer film casting, the reader may wish to consult Middleman [7], Agassant *et al.* [8] and Kumar *et al.* [9].

The film casting of two- and multi-layer flows is essentially unexplored. The theoretical analyses are very limited. Park [4] performed the first theoretical analysis on two-layer film casting. Using simple constitutive models, Park investigated the effects of the interaction between two fluids with different rheological properties on the film thickness and stress profiles. One layer was Newtonian and the second was an upper-convected-Maxwell fluid. Two limiting cases, namely fluids with small elasticity, and fluids with large applied tension at the take-up point, were studied. In the case of the two-layer flow with small elasticity, the film thickness and velocity profile were found to be similar to those for a Newtonian single-layer film. In the case of a large applied tension at the take-up point, the velocity was shown to increase linearly with axial position. It was found that the Maxwell layer dictated the mechanics of the flow, even when its flow rate and shear viscosity were much smaller than those of the Newtonian layer. All results were obtained based on an asymptotic analysis, in which a small parameter ε defined as the ratio of the two characteristic length scales across and along the film direction was applied. At the leading order in ε, the axial velocity along the direction of drawing (see Figure 1), is dependent on x only. Consequently, the axial velocities of the two layers are found to be uniform by employing the condition of the continuity of the axial velocity at the interface. Co *et al.* [5, 6] adopted a similar assumption and studied the multi-layer film casting of modified Giesekus fluids. Assuming the axial velocity is uniform across the whole film thickness, Co *et al.* investigated the effects of the rheological properties of each layer and draw ratio on the steady-state flow [5] and the instability [6]. In the stability analysis, the eigenvalue problem was treated as a two-boundary problem. The numerical simulation method is similar to the shooting method used by Yeow [1] in his linear stability analysis of single-layer film casting. The results indicate that the layer with a much larger elongational viscosity dominates the overall flow behaviour, even if its thickness fraction is small. The critical draw ratios for two-layer films of various thickness fractions are bounded by those for single-layer films of the two fluids. Extensional-thickening has a stabilizing effect, whereas shear-thinning and extensional-thinning have destabilizing effects.

The interaction of the fluids in multi-layer flow is complicated, and cannot be ascertained without some simplifying assumptions. All the previous studies on film casting, either single- or multi-layer flow, assume that the flow is predominantly elongational, i.e. the velocity gradient is linear along the direction of the flow, resulting in a dominant axial velocity that is uniform across the thickness. Under this assumption, the boundary conditions at the interface between two layers, namely the continuity of the axial velocity and the traction, cannot be simultaneously accommodated. Thus either the velocity or the traction can be continuous across the interface. However, the imposition of a continuous velocity vector across the interface is erroneous for three major reasons. First, the continuity of the velocity results in the same axial velocity component across the entire film, regardless of the viscosity ratio of the two layers. Second, in the real two-layer film casting process, and unlike single-layer film flow, there is bound to be a certain amount of shearing that increases with the viscosity ratio. In this case, the axial velocity cannot be (even approximately) uniform across the entire film. In fact, in the limit of zero or infinite viscosity ratio, one of the layers is effectively a solid, resulting in the formation of a boundary layer. Third, there may be a considerable slip at the

interface. Consider, for instance, the case where the fluid in contact with the chill roll is the less viscous layer. Since the flow in this layer is predominantly elongational, it may fail to fully entrain the second layer, resulting in slip.

In the present study, the continuity of traction is ensured at the interface, and the axial velocity is assumed to be uniform across each film layer separately. Generally, the velocities in the two layers are not the same. It is easy to anticipate that the flow of the two-layer film will be different from the flow of a single-layer film. The difference becomes greater if the rheological properties of the two layers are more different from one another. The major objective of this study is to investigate how the mechanics of the two-layer film casting flow and its stability are affected by the properties of each layer. Inertia and gravity effects, which were neglected in the previous works, are also examined. The study focuses on stability analysis and steady-state two-layer Newtonian film casting. The influence of inertia, fluid properties such as viscosity ratio and density ratio, as well as processing conditions such as velocity ratio and thickness ratio, on the critical draw ratio will be investigated. Also, the effects of inertia, gravity, fluid properties as well as processing conditions, on the steady-state flow will be examined.

2. FORMULATION OF GOVERNING EQUATIONS

In this section, the general formulation is discussed for two-layer film casting as depicted in Figure 1. In the film casting process, the width of the film is very large compared with its thickness and often much larger than the distance between the die and the chill roll (air gap); the film contraction in the width direction (neck-in) can hence be neglected, and the flow can be considered as two-dimensional. The die swell, i.e. the phenomenon of the film thickness increasing after being extruded from the die, is also ignored, considering the variation of the film thickness is small. Although the film is air cooled, the flow is assumed to be isothermal since most of cooling happens at the take-up point.

Consider the two-layer film flow, Newtonian and incompressible fluid, of layer a and layer b with different densities ρ^{a} and ρ^{b}, and viscosities μ^{a} and μ^{b}, respectively. The velocity is assumed to be uniform across each layer separately, so that the velocities of the two layers, u^{a} and u^{b}, are functions only of the streamwise position x and time t. Under these assumptions and in the presence of inertia and gravity forces, the conservations of mass and momentum reduce, respectively, to

$$u^i_{,x} + v^i_{,y} = 0 \tag{1}$$

$$\rho^i(u^i_{,t} + u^i u^i_{,x}) = \sigma^i_{xx,x} + \sigma^i_{xy,y} + \rho^i g \tag{2}$$

where i refers to layer a or b, and a subscript after a comma denotes partial differentiation. Here σ_{xx} and σ_{xy} are the normal and shear stress, respectively, g is the gravitational acceleration, and t is the time.

The boundary conditions are prescribed as follow. At the die exit and the chill roll, the velocities in the draw direction are given as

$$u^{\mathrm{a}}(t, x=0) = u^{\mathrm{a}}_0, \quad u^{\mathrm{b}}(t, x=0) = u^{\mathrm{b}}_0, \quad u^{\mathrm{a}}(t, x=L) = u^{\mathrm{a}}_L \tag{3}$$

where the air gap length, L, is the length from the die exit to the chill roll. The film thickness of each layer at $x=0$ is given as

$$\delta^{\mathrm{a}}(t,x=0)=\delta_0^{\mathrm{a}},\quad \delta^{\mathrm{b}}(t,x=0)=\delta_0^{\mathrm{b}} \tag{4}$$

where δ^{a} and δ^{b} are the film thickness of layer a and layer b, respectively. The tractions of the two layers, $\mathbf{t}^{\mathrm{a}}$ and $\mathbf{t}^{\mathrm{b}}$, are held equal at the interface:

$$\mathbf{t}^{\mathrm{a}}(t,y=h^{\mathrm{f}})=\mathbf{t}^{\mathrm{b}}(t,y=h^{\mathrm{f}}) \tag{5}$$

where h^{f} is the interface height.

Noting that the molten polymer has a high viscosity and the film thickness varies slowly, surface tension and air drag are assumed to be negligible, leading to the following dynamic conditions on the free surfaces:

$$\mathbf{t}^{\mathrm{a}}(t,y=h^{\mathrm{a}})=0,\quad \mathbf{t}^{\mathrm{b}}(t,y=h^{\mathrm{b}})=0 \tag{6}$$

where h^{a} and h^{b} are the two free surface heights. The film thickness of layer a and layer b are δ^{a} and δ^{b}, respectively. Thus

$$\delta^{\mathrm{a}}=h^{\mathrm{f}}-h^{\mathrm{a}},\quad \delta^{\mathrm{b}}=h^{\mathrm{b}}-h^{\mathrm{f}} \tag{7}$$

If the momentum equation in each layer is integrated across the layer, and Equations (5)–(7) are used, then the following equation for the velocity is obtained.

$$\begin{aligned}&(\rho^{\mathrm{a}}\delta^{\mathrm{a}}+\rho^{\mathrm{b}}\delta^{\mathrm{b}}R_\mu)u^{\mathrm{a}}_{,t}+(\rho^{\mathrm{a}}\delta^{\mathrm{a}}+\rho^{\mathrm{b}}\delta^{\mathrm{b}}R_\mu^2)u^{\mathrm{a}}u^{\mathrm{a}}_{,x}+\rho^{\mathrm{b}}\delta^{\mathrm{b}}R_\mu(u_0^{\mathrm{b}}-R_\mu u_0^{\mathrm{a}})u^{\mathrm{a}}_{,x}\\&\quad=4\mu^{\mathrm{a}}(\delta^{\mathrm{a}}+\delta^{\mathrm{b}})u^{\mathrm{a}}_{,xx}+4\mu^{\mathrm{a}}(\delta^{\mathrm{a}}_{,x}+\delta^{\mathrm{b}}_{,x})u^{\mathrm{a}}_{,x}+(\delta^{\mathrm{a}}\rho^{\mathrm{a}}+\delta^{\mathrm{b}}\rho^{\mathrm{b}})g\end{aligned} \tag{8}$$

where R_μ denotes the viscosity ratio of layer a to layer b. Note here that condition (5), together with the fact that the normal components of the interface satisfy $n_y \gg n_x$, lead to

$$\mu^{\mathrm{a}}u^{\mathrm{a}}_{,x}=\mu^{\mathrm{b}}u^{\mathrm{b}}_{,x} \tag{9}$$

Combining the kinematic condition and the continuity equation at the free surface gives

$$\delta^{\mathrm{a}}_{,t}+(u^{\mathrm{a}}\delta^{\mathrm{a}})_{,x}=0 \tag{10}$$

$$\delta^{\mathrm{b}}_{,t}+(u^{\mathrm{b}}\delta^{\mathrm{b}})_{,x}=0 \tag{11}$$

It is convenient to cast the problem in dimensionless form. Thus, L will be taken as the reference length, u_0^{a} the reference velocity, and δ_0^{a} the reference thickness. The dimensionless variables of relevance to the problem are then defined as follows

$$X=\frac{x}{L},\quad T=\frac{u_0^{\mathrm{a}}}{L}t,\quad U^i=\frac{u^i}{u_0^{\mathrm{a}}},\quad \Delta^i=\frac{\delta^i}{\delta_0^{\mathrm{a}}} \tag{12}$$

In this case, seven parameters emerge in the problem, namely the draw ratio, D_{R}, the thickness ratio, R_δ, the velocity ratio, R_u, the density ratio R_ρ, the viscosity ratio R_μ, the Froude number

Fr, as well as the Reynolds number, Re, which are introduced as

$$R_\delta = \frac{\delta_0^{\mathrm{b}}}{\delta_0^{\mathrm{a}}}, \quad R_u = \frac{u_0^{\mathrm{b}}}{u_0^{\mathrm{a}}}, \quad R_\rho = \frac{\rho^{\mathrm{b}}}{\rho^{\mathrm{a}}}, \quad R_\mu = \frac{\mu^{\mathrm{a}}}{\mu^{\mathrm{b}}}$$

$$D_{\mathrm{R}} = \frac{u_L^{\mathrm{a}}}{u_0^{\mathrm{a}}}, \quad Fr = \frac{u_0^{\mathrm{a}^2}}{gL}, \quad Re = \frac{\rho^{\mathrm{a}} u_0^{\mathrm{a}} L}{\mu^{\mathrm{a}}}$$

In dimensionless form, Equations (8)–(11) are written as

$$Re\lfloor(\Delta^{\mathrm{a}} + R_\rho R_\mu \Delta^{\mathrm{b}})U^{\mathrm{a}}_{,T} + (\Delta^{\mathrm{a}} + R_\rho R_\mu^2 \Delta^{\mathrm{b}})U^{\mathrm{a}} U^{\mathrm{a}}_{,X} + R_\rho R_\mu (R_u - R_\mu)\Delta^{\mathrm{b}} U^{\mathrm{a}}_{,X}\rfloor$$

$$= 4(\Delta^{\mathrm{a}} + \Delta^{\mathrm{b}})U^{\mathrm{a}}_{,XX} + 4(\Delta^{\mathrm{a}}_{,X} + \Delta^{\mathrm{b}}_{,X})U^{\mathrm{a}}_{,X} + \frac{Re}{Fr}(\Delta^{\mathrm{a}} + R_\rho \Delta^{\mathrm{b}}) \tag{13}$$

$$\Delta^{\mathrm{a}}_{,T} + (\Delta^{\mathrm{a}} U^{\mathrm{a}})_{,X} = 0 \tag{14}$$

$$\Delta^{\mathrm{b}}_{,T} + (\Delta^{\mathrm{b}} U^{\mathrm{b}})_{,X} = 0 \tag{15}$$

$$U^{\mathrm{b}} = R_\mu U^{\mathrm{a}} - R_\mu + R_u \tag{16}$$

The boundary conditions become

$$\Delta^{\mathrm{a}}(T, X = 0) = 1, \quad \Delta^{\mathrm{b}}(T, X = 0) = R_\delta \tag{17}$$

$$U^{\mathrm{a}}(T, X = 0) = 1, \quad U^{\mathrm{a}}(T, X = 1) = D_{\mathrm{R}} \tag{18}$$

3. STEADY TWO-LAYER FLOW

In this section, the steady flow is examined. The solution procedure is first discussed, and the influence of various flow parameters is then investigated on the steady-state solution.

3.1. Solution procedure

The steady-state flow is a problem of the two-point boundary-value type, which is governed by a set of ordinary differential equations (ODEs), subject to constraints at the endpoints of the interval $X \in [0, 1]$. The problem is solved based on the IMSL (International Mathematical and Statistical Libraries) FORTRAN numerical library sub-routine DBVPFD, which solves a system of differential equations with boundary conditions at two points, using a variable order, variable step size finite-difference method with deferred corrections. The basic discretization is the trapezoidal rule over a non-uniform mesh. The mesh is chosen adaptively, to make the local error approximately the same size everywhere. The sub-routine keeps the global error estimates smaller than the user-specified tolerance. A step size (Δx) less than 0.01 was used to maintain a tolerance of 10^{-7}.

For steady flow, the layer thickness of each layer can be expressed in terms of the velocity of the layer from Equations (14) and (15). Thus, upon using Equation (16), one obtains

$$\Delta^{\mathrm{as}} = \frac{1}{U^{\mathrm{as}}}, \quad \Delta^{\mathrm{bs}} = \frac{R_\delta R_u}{R_\mu U^{\mathrm{as}} - R_\mu + R_u} \tag{19}$$

where the superscripts, as and bs, denote steady-state variables of layer a and layer b, respectively.

In this case, the solution process reduces to the integration of the following equation for $U^{as}(X)$

$$Re\lfloor(\Delta^{as}+R_\rho R_\mu^2\Delta^{bs})U^{as}U^{as}_{,X}+R_\rho R_\mu(R_u-R_\mu)\Delta^{bs}U^{as}_{,X}\rfloor$$
$$=4(\Delta^{as}+\Delta^{bs})U^{as}_{,XX}+4(\Delta^{as}_{,X}+\Delta^{bs}_{,X})U^{as}_{,X}+\frac{Re}{Fr}(\Delta^{as}+R_\rho\Delta^{bs}) \tag{20}$$

which must be solved subject to the conditions:

$$U^{as}(X=0)=1,\quad U^{as}(X=1)=D_R \tag{21}$$

Note that given the nonlinear nature of the problem, a Newton's iteration method with step control is used for the solution.

3.2. *Discussion and results*

In this section, the formulation and the numerical solution are applied to the two-layer film casting flow as schematically illustrated in Figure 1. The velocity profiles, the film thickness distributions and the axial forces along the film length as well as the draw forces at the take-up point for each layer will be determined. The influence of inertia and gravity, the properties of the fluid (viscosity and density ratios), and the processing condition (draw ratio), on the flow are investigated. All the results are given in terms of dimensionless quantities.

3.2.1. Influence of inertia. The influence of inertia on the two-layer film casting flow is investigated by varying the Reynolds number over the range $Re\in[0,2]$ while the other parameters of the flow are fixed. In this case, the draw ratio, D_R, the viscosity ratio, R_μ, and the density ratio, R_ρ, are set equal to 12, 2 and 0.4, respectively. The film thickness and velocity ratios at the die exit ($X=0$), R_δ and R_u, as well as the Froude number, Fr, are all set equal to 1. Since the effect of gravity on the single layer steady-state flow is opposite to that of inertia [10], in order to highlight the influence of inertia, the effect of gravity is chose sufficiently small, $Fr=1$. This is based on the fact (obtained by extensional calculations) that, under the fixed values of the other parameters, the flow response to $Fr=1$ is almost the same as $Fr\to\infty$ (also see Figure 10), which means the gravity effect is negligible. The flow response is depicted in Figures 2–4, where the two-layer velocity distributions, $U^{as}(X)$ and $U^{bs}(X)$, the thickness, $\Delta^{as}(X)$ and $\Delta^{bs}(X)$, and the axial forces, $F^{as}(X)$ and $F^{bs}(X)$, in each layer are plotted against X. The draw forces at the take-up point, $F^{as}(X=1)$ and $F^{bs}(X=1)$, are also plotted vs Re in Figure 4.

The results show that the velocity increases monotonically with X in each layer, at a rate that is relatively slower (faster) near the die exit (take-up point) as Re increases. The velocity of each layer at the take-up point is independent of inertia. While this observation is of course expected for layer a because of boundary condition (18), it is less obvious regarding layer b. However, this is also confirmed from relation (16), which shows that $U^{bs}(X=1)=R_\mu D_R-R_\mu+R_u$ is indeed independent of Re.

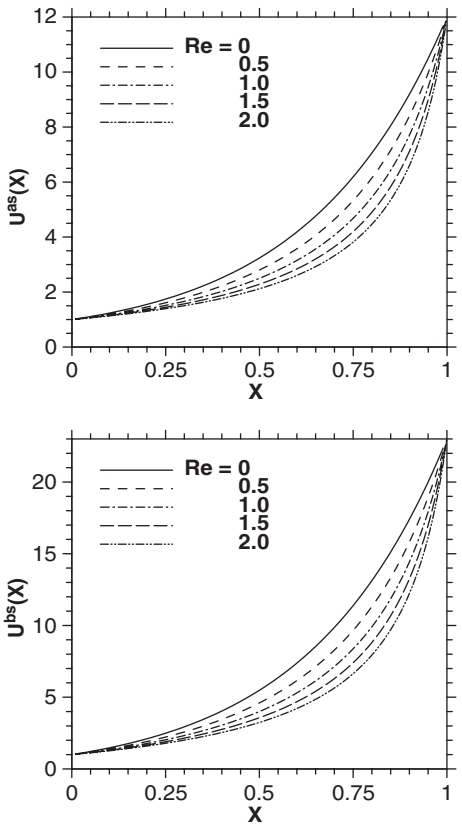

Figure 2. Influence of inertia on the velocities, $U^{as}(X)$ and $U^{bs}(X)$, for $Re \in [0, 2]$, $D_R = 12$, $R_\mu = 2$, $R_\rho = 0.4$, $R_\delta = R_u = Fr = 1$.

It is important to also observe that the velocity distribution along each layer deviates from the exponential behaviour that is typical of creeping flow of single-layer films [1, 7, 10]. In the absence of inertia, the following analytical equation is obtained for U^{as}:

$$(U^{as})^{\frac{R_\mu}{R_\delta R_u}} \left(U^{as} + \frac{R_u}{R_\mu} - 1 \right) = \frac{R_u}{R_\mu} e^{X \ln \left[\frac{R_\mu}{R_u} D_R^{\frac{R_\mu}{R_\delta R_u}} \left(D_R + \frac{R_u}{R_\mu} - 1 \right) \right]} \tag{22}$$

Equation (22) is obtained by setting $Re = 0$, substituting Equation (19) into Equation (20), integrating the resulting equation with respect to X from 0 to 1, and applying the boundary condition (21). Clearly, Equation (22) indicates that exponential behaviour is never encountered for two-layer films, even at zero Reynolds number, except when the ratio $R_u/R_\mu = 1$. In this case, $U^{as} = D_R^X$ and $U^{bs} = R_\mu D_R^X$. The corresponding thickness in each layer in this case is given by $\Delta^{as} = D_R^{-X}$ and $\Delta^{bs} = R_\delta D_R^{-X}$. This is an interesting result as it shows that, in the absence of inertia, as long as the velocity ratio is equal to the viscosity ratio at the die exit, the flow velocity and film thickness in layer a are exactly the same as those for a single-layer

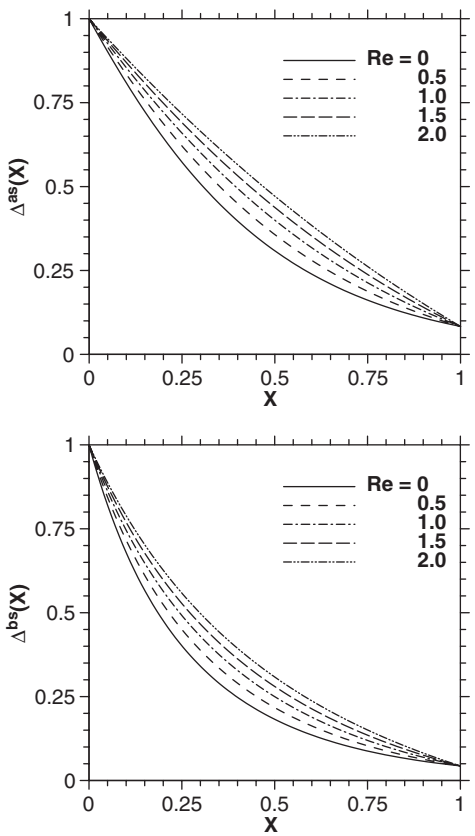

Figure 3. Influence of inertia on the film thickness, $\Delta^{as}(X)$ and $\Delta^{bs}(X)$, for $Re \in [0,2]$, $D_R = 12$, $R_\mu = 2$, $R_\rho = 0.4$, $R_\delta = R_u = Fr = 1$.

film, and the velocity and thickness in layer b are larger by a factor equal to the viscosity ratio and thickness ratio at the die exit, respectively. More generally, in the presence of inertia, although the velocity and thickness of each layer at the take-up point are independent of inertia, the overall velocity and thickness deviate from exponential behaviour as Re increases, reflecting an intensification of the nonlinear character of the flow. It should be pointed out that the velocity profile and the film thickness distribution along the X direction coincide with those of the single-layer film casting [10], if the flow parameters in the two-layer problem are chose such that $R_\mu = R_\rho = R_u = 1$. In fact, in this case, $U^s = D_R^X$ and $\Delta^s = D_R^{-X}$, which are identical to References [7, 10] for single-layer film casting.

Consider now the axial force distribution. Recall that this is the only non-zero force component, and is expected to be dominant in practice. In this problem, a suitable force scale is taken as $\mu^a \delta_0^a u_0^a / L$, and the dimensionless axial forces in layers a and b become $F^{as}(X) = 4U_X^{as}\Delta^{as}$ and $F^{bs}(X) = 4U_X^{as}\Delta^{bs}$, respectively. It is observed from Figure 4 that inertia has a significant effect on the axial forces. The magnitude of the axial force in each layer decreases slowly near the die exit, and increases sharply near the take-up point, as Re increases. The variation

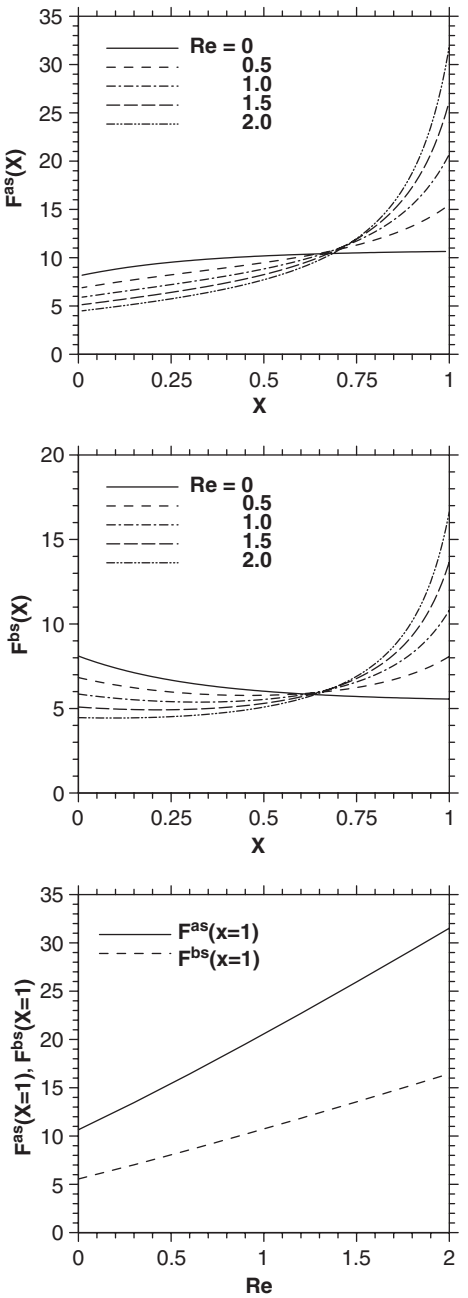

Figure 4. Influence of inertia on the draw forces, for $Re \in [0,2]$, $D_R = 12$, $R_\mu = 2$, $R_\rho = 0.4$, $R_\delta = R_u = Fr = 1$. The figure shows the axial forces, $F^{as}(X)$ and $F^{bs}(X)$, along the draw direction and the draw forces at the take up point ($X = 1$), $F^{as}(X = 1)$ and $F^{bs}(X = 1)$, against the Reynolds number.

of the force is not always monotonic with respect to X. Indeed, for creeping flow ($Re = 0$), $F^{as}(X)$ increases with X, while $F^{bs}(X)$ decreases with X, but both tend to an asymptotic level near the take-up point. In fact, in the absence of inertia, Equation (13) can be written as $(U_X^{as}\Delta^{as} + U_X^{as}\Delta^{bs})_X = 0$, which indicates that the sum of the two forces is unchanged along the film direction. Note that the force in a single-layer film is constant everywhere [7]. For small but non-zero Re, the force in layer a increases monotonically with X, at a rate that increases with Re. The force in layer b exhibits a minimum that weakens with Re. For $Re > 1$, the axial forces of both layers increase monotonically with X, relatively slowly near the die exit, and sharply near the take-up point.

It is particularly important to examine the influence of inertia on the force in each layer at the take-up point, and these are also shown in Figure 4. Unlike the velocity and the film thickness, the draw forces at the take-up point depend significantly on inertia, and increase almost linearly with Re for both layers. This suggests that in practice, films with higher inertia require more draw force to achieve the same draw ratio and film thickness.

3.2.2. Influence of viscosity ratio. The effect of viscosity on the velocities, the film thickness and the axial forces is explored by examining the two-layer film casting flow for different values of the viscosity ratio, $R_\mu \in [1, 5]$. The remaining parameters are fixed at $D_R = 12$, $Fr = Re = 1$, $R_\rho = 0.4$, $R_\delta = R_u = 1$. The flow response is depicted in Figures 5–7.

It is observed that the velocity in each layer increases monotonically with X, regardless of R_μ, but the elongation rate depends strongly on R_μ and is different for each layer. As R_μ increases, the overall velocity decreases in layer a and increases in layer b, which of course suggests that the flow in layer a weakens as the layer becomes relatively more viscous, leaving layer b to flow at a faster rate (see Figure 5). It is expected that as R_μ increase further, the flow activity in layer a becomes increasingly limited to the region near the take-up point, with the layer behaving more like a solid almost everywhere except at the tip where considerable stretching occurs. Simultaneously, the draw ratio, D_R^b, in layer b increases with R_μ. This suggests that, in practice, the draw ratio in layer b must be increased with increasing viscosity ratio to make the casting process achievable. However, this makes the process more vulnerable to instability. The dependence of D_R^b on the flow parameters is plotted in Figure 5, but can be inferred from Equation (16), which, in the present case, reduces to

$$D_R^b = R_\mu D_R - R_\mu + 1 \tag{23}$$

Equation (23) indicates that the draw ratio for layer b, D_R^b, is independent of density ratio, R_ρ, and equals to the draw ratio for layer a, D_R, at $R_\mu = 1$. This is confirmed in Figure 5.

The overall thickness of layer a increases with R_μ, while the overall thickness of layer b decreases (Figure 6). Although the thickness of layer b at the take-up point is independent of inertia (Figure 3), it depends strongly on R_μ. Figure 6 displays the dependence of $\Delta^{bs}(X = 1)$ on the viscosity ratio for various values of the draw ratio. The results show that the thickness decreases with both parameters, $\Delta^{bs}(X = 1) \approx 1/D_R R_\mu$ for the current remaining parameters.

The force distributions in each layer (Figure 7) show that the influence of the viscosity ratio is not always uniform. While the force in layer b decreases everywhere with viscosity ratio, the force in layer a decreases only near the die exit, and increases sharply at the take-up point. Two interesting observations can be made here. The first being the non-monotonicity of $F^{bs}(X)$, as it displays a minimum for the higher viscosity ratios. The second observation is that while the thickness in each layer changes little with viscosity ratio, the force in the less

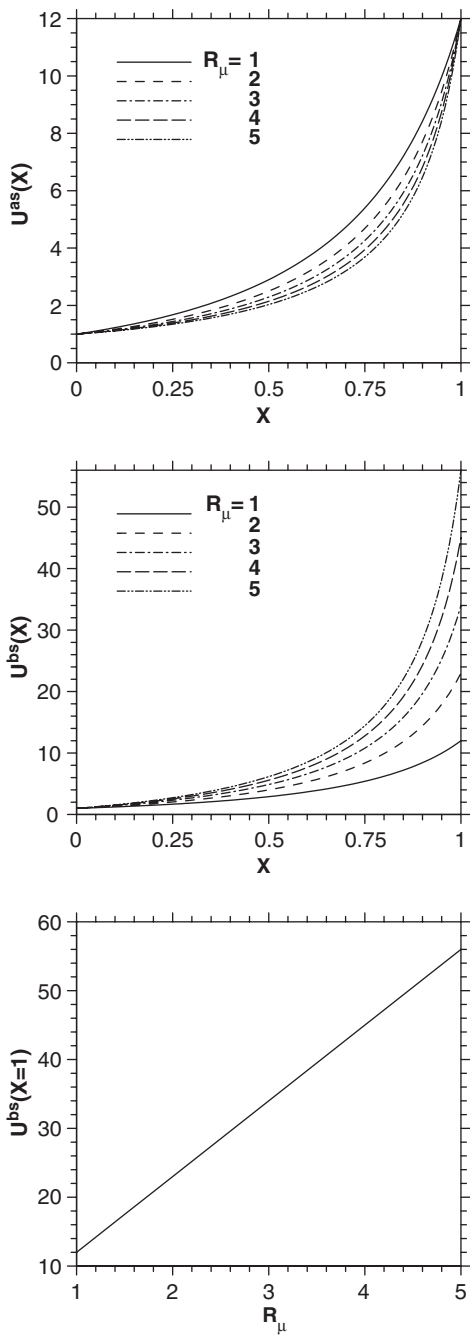

Figure 5. Influence of viscosity ratio on the velocities, for $R_\mu \in [1,5]$, $D_R = 12$, $R_\rho = 0.4$, $Re = Fr = R_\delta = R_u = 1$. The figure shows the velocity profiles, $U^{as}(X)$ and $U^{bs}(X)$, along X direction, and the velocity of layer b at the take-up point, $U^{bs}(X = 1)$, vs the viscosity ratio R_μ.

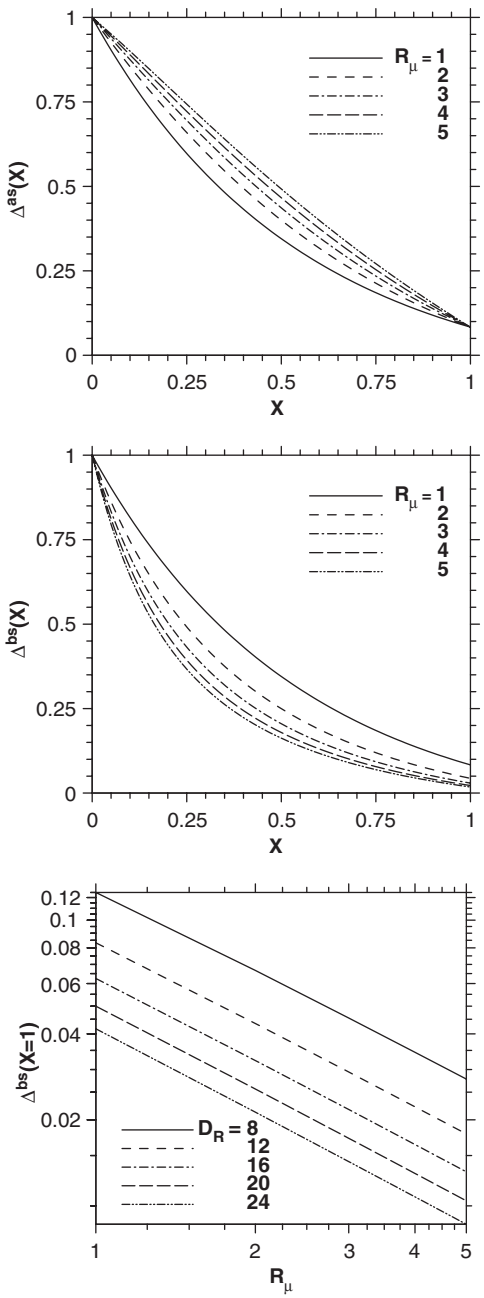

Figure 6. Influence of viscosity ratio on the film thickness, for $R_\mu \in [1,5]$, $R_\rho = 0.4$, $Re = Fr = R_\delta = R_u = 1$. The figure shows the film thickness distributions, $\Delta^{as}(X)$ and $\Delta^{bs}(X)$, along X direction for $D_R = 12$, and the film thickness of layer b at the take-up point, $\Delta^{bs}(X = 1)$, vs the viscosity ratio R_μ in log–log scale for $D_R \in [8, 24]$.

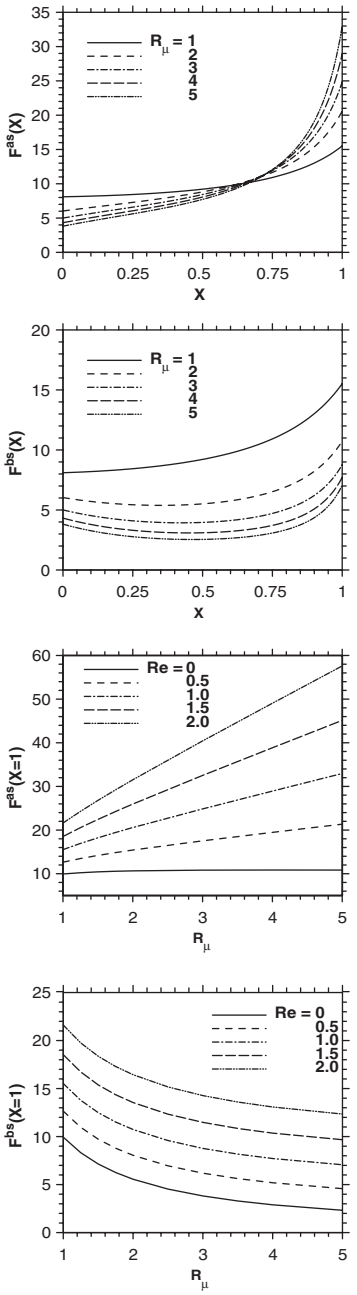

Figure 7. Influence of viscosity ratio on the axial forces, for $R_\mu \in [1,5]$, $D_R = 12$, $R_\rho = 0.4$, $Re = Fr = R_\delta = R_u = 1$. The figure shows axial force distributions, $F^{as}(X)$ and $F^{bs}(X)$, along X direction, and the draw forces at the take-up point, $F^{as}(X=1)$ and $F^{bs}(X=1)$, vs the viscosity ratio R_μ for different Re.

viscous layer, b (see Figure 7, for $R_\mu = 5$), is reduced substantially despite the strong buildup of elongational effects (see Figure 6).

The forces at the take-up point in each layer are also plotted in Figure 7 against R_μ for different values of Re. While the draw force increases in layer a with the viscosity ratio, it decreases in layer b. This further confirms the stronger need for drawing of layer a, as the force increases essentially linearly with the viscosity ratio. The slope depends on the level of inertia, and is estimated to increase like $4.3Re$. Note that the rate of decrease of the force in layer b is essentially independent of Re.

3.2.3. Influence of density ratio. Consider now the influence of the density ratio on the flow, which is examined by varying R_ρ from 1 to 5. In this case $D_R = 12$, $R_\mu = 2$, and $Re = Fr = R_u = R_\delta = 1$. The flow response is depicted in Figures 8 and 9. Only results with new features are reported in these figures. It is interesting to note, at the outset, that if all the fluid parameters are equal in layers a and b, the resulting velocity, thickness and force distributions would be the same as those corresponding to single-layer film casting even when the densities in the two layers are not equal. The velocity distributions are very similar to those in Figure 2. The velocity in both layers decreases with the density ratio, which suggests that increasing the density ratio enhances elongational effects in both layers. The flow elongation is strong enough to halt the decrease of the film thickness in layer a with X. Although the velocity and thickness at the take-up point in each layer are not affected by R_ρ, the drawing force depends strongly on the density ratio. The force in each layer increases monotonically with X similarly to Figure 4 ($Re \neq 0$). Figure 9 indicates, as expected, that the density ratio has no effect on the flow in the absence of inertia. Generally, the draw force in both layers increases linearly with R_ρ, suggesting a larger drawing force is needed for a heavier fluid. The slopes in layer a and b increase like $13.2Re$ and $6.8Re$, respectively.

3.2.4. Influence of gravity. The effect of gravity is examined by varying the Froude Number, Fr. Figure 10 displays the force distributions as well as the take-up force in each layer over the range $Fr \in [0.01, \infty)$, with the remaining parameters fixed at $D_R = 12$, $Re = 1$, $R_\mu = 2$, $R_\rho = 0.4$, $R_\delta = 1$ and $R_u = 1$. Only the forces are shown because the velocity and thickness profiles do not exhibit any new qualitative features in comparison to Figures 2 and 3. Indeed, it is found that both velocity and film thickness at the take-up point are independent of Fr. However, the overall velocity in both layers increases due to gravity, deviating gradually from the exponential growth to grow linearly with X as Fr decreases. Simultaneously, the film thickness begins to decrease rather sharply near the die exit as gravity increases.

Gravity is found to have a dramatic effect on the axial forces in both layers, as depicted in Figure 10. In the absence of gravity or for relatively large Froude number, the force in layer a increases monotonically with X, whereas the force in layer b exhibits a weak minimum. As the effect of gravity increases, the forces in both layers show a minimum that strengthens with gravity, and is located closer to the take-up point. It is interesting to observe that while the two layers have very different fluid parameters (layer a is twice as viscous as layer b), the overall force magnitude is the same in both layers, particularly near the die exit, where, incidentally, the effect of gravity is most influential; there is a sharp jump in the force value as Fr increases, reflecting a significant buildup in elongational effect at the die exit. However, the work done by the force in each layer to move the fluid from the die exit to the take-up point is unaffected by gravity; the area below the curves $F^{as}(X)$ and $F^{bs}(X)$ is unchanged as

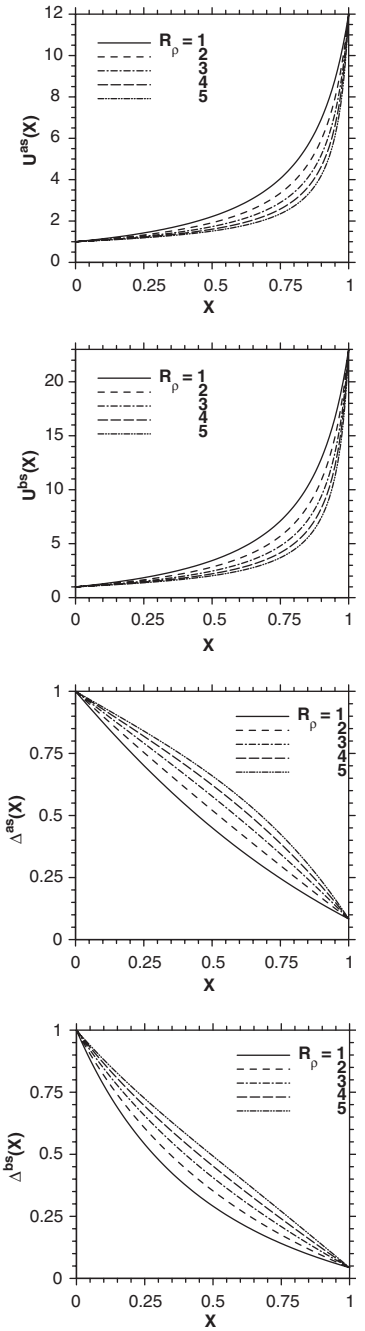

Figure 8. Influence of density ratio on the two-layer film flow, for $R_\rho \in [1,5]$, $D_R = 12$, $R_\mu = 2$, $Re = Fr = R_\delta = R_u = 1$. The figure shows the velocity profiles, $U^{as}(X)$ and $U^{bs}(X)$, the film thickness distributions, $\Delta^{as}(X)$ and $\Delta^{bs}(X)$, along X direction.

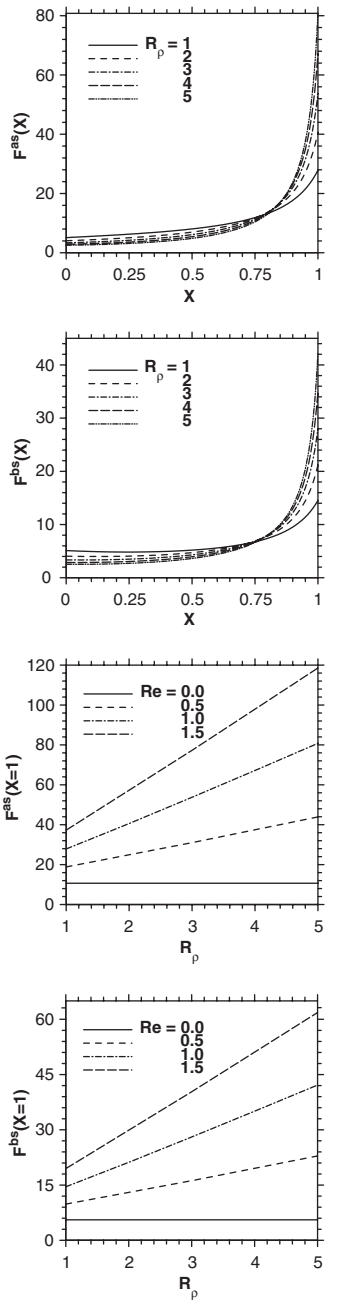

Figure 9. Influence of density ratio on the axial forces and draw forces, for $R_\rho \in [1, 5]$, $D_R = 12$, $R_\mu = 2$, $Re = Fr = R_\delta = R_u = 1$. The figure shows axial force distributions, $F^{as}(X)$ and $F^{bs}(X)$, along X direction, and the draw forces at the take-up point, $F^{as}(X = 1)$ and $F^{bs}(X = 1)$, vs the density ratio R_ρ for different Re.

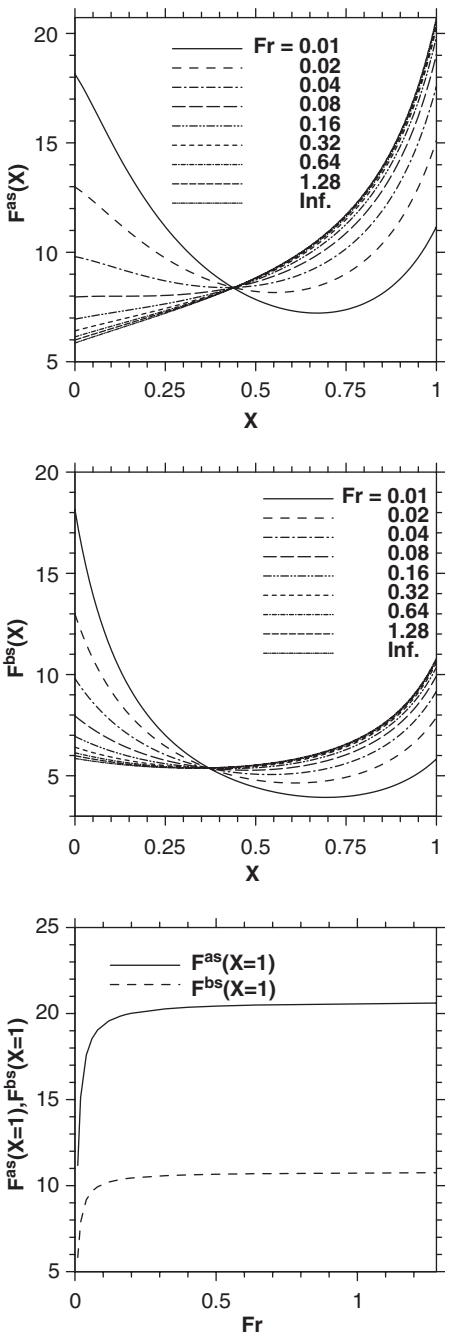

Figure 10. Influence of gravity on the axial forces and draw forces, for $Fr \in [0.01, \infty]$, $D_R = 12$, $R_\mu = 2$, $R_\rho = 0.4$, $Re = R_\delta = R_u = 1$. The figure shows axial force distributions, $F^{as}(X)$ and $F^{bs}(X)$, along X direction, and the draw forces at the take-up point, $F^{as}(X = 1)$ and $F^{bs}(X = 1)$, vs Fr.

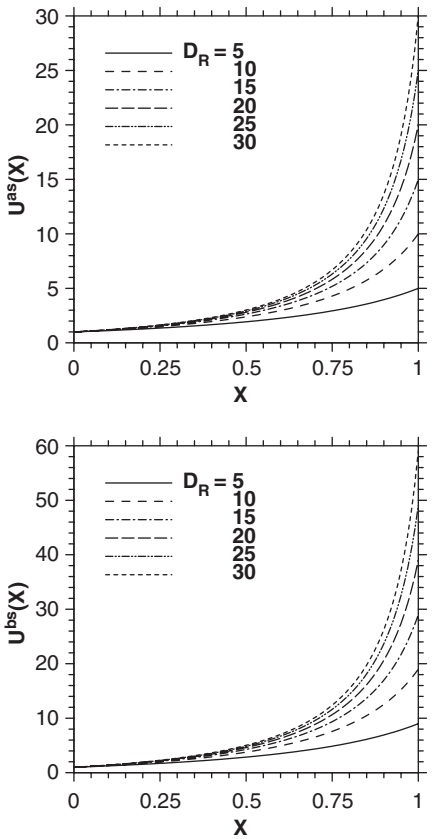

Figure 11. Influence of draw ratio on the velocities, for $D_R \in [5, 30]$, $R_\mu = 2$, $R_\rho = 0.4$, $Re = Fr = R_\delta = R_u = 1$. The figure shows the velocity profiles, $U^{as}(X)$ and $U^{bs}(X)$, along X direction, and the velocities at the take up point, $U^{as}(X = 1)$ and $U^{bs}(X = 1)$, against draw ratio D_R.

Fr varies. This is easily confirmed from the expression of the work, W^{as} and W^{bs}, in layer a and b, respectively, which can be obtained by integrating the axial forces $F^{as}(X)$ and $F^{bs}(X)$ with respect X from 0 to 1, making use of Equations (19) and (21). The expressions for W^{as} and W^{bs} are given in closed form, namely

$$W^{as} = 4\ln(D_R) \quad \text{and} \quad W^{bs} = \frac{4R_u R_\delta}{R_\mu} \ln\left(\frac{R_\mu}{R_u} D_R - \frac{R_\mu}{R_u} + 1\right) \tag{24}$$

which clearly shows the work done in each layer is independent of gravity.

The draw force at the take-up point decreases dramatically with gravity. The figure shows that both $F^{as}(X = 1)$ and $F^{bs}(X = 1)$ increase sharply with Fr but tend to level off as Fr goes to infinity. This indicates that, at the take-up point, the draw force in each layer required to achieve the same draw ratio becomes smaller due to the increasing effect of gravity. The decrease in draw force at the take-up point, and the increase in the force at the die exit, as gravity effect increases, is now not difficult to understand in the light of expressions (24).

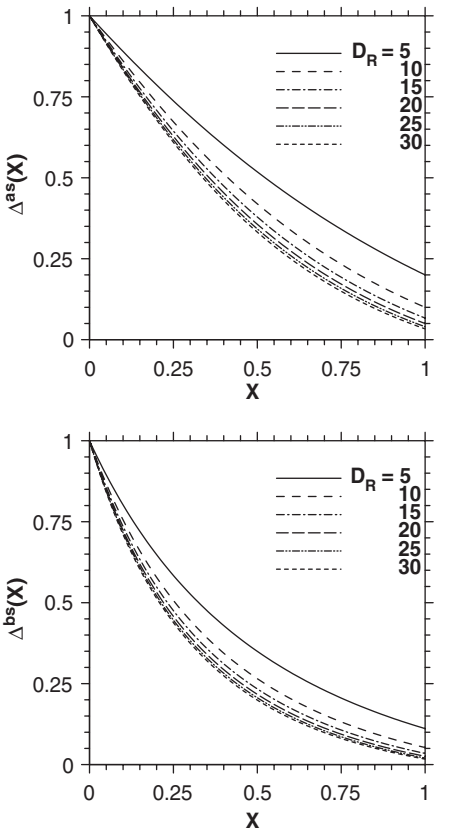

Figure 12. Influence of draw ratio on the film thickness, for $D_R \in [5, 30]$, $R_\mu = 2$, $R_\rho = 0.4$, $Re = Fr = R_\delta = R_u = 1$. The figure shows the film thickness distributions, $\Delta^{as}(X)$ and $\Delta^{bs}(X)$, along X direction, and the film thickness at the take up point, $\Delta^{as}(X = 1)$ and $\Delta^{bs}(X = 1)$, against draw ratio D_R.

3.2.5. Influence of draw ratio. So far, the study has focused on the influence of the fluid properties on the two-layer film flow. In the film casting process, the important parameters, which describe the system, are the length from the die exit to the chill roll (air gap), L, and the draw ratio, D_R, which is the ratio of the take-up velocity at the chill roll to the extrusion velocity at the die exit. The effect of L has already been examined through the influence of the Reynolds number. For incompressible fluids, D_R is equal to the ratio of the thickness of the film leaving the die to the thickness of the film at the chill roll. To examine the effect of the draw ratio, consider the velocity, the film thickness and axial forces in each layer for draw ratios in the range from 5 to 30. The velocities, the film thickness and the draw forces at the take-up point are also examined against the draw ratio for different levels of inertia. In this case, the viscosity ratio and density ratio are set equal to 2 and 0.4, respectively; the remaining parameters are set equal to 1. The results are shown in Figures 11–13.

Overall, the velocity, film thickness and axial force distributions are sensitive to D_R, but the influence of the draw ratio is strongest near the take-up point. The velocity and draw force

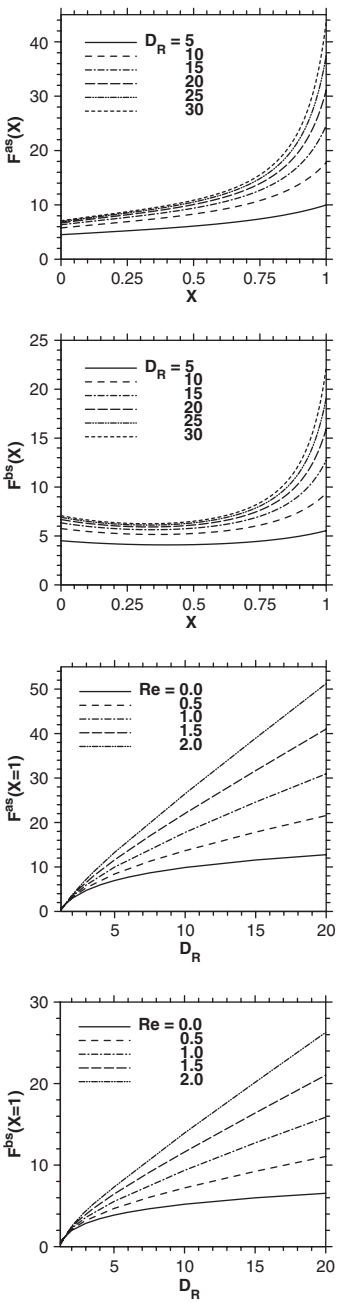

Figure 13. Influence of draw ratio on the axial forces and draw forces, for $D_{\mathrm{R}} \in [5, 30]$, $R_\mu = 2$, $R_\rho = 0.4$, $Re = Fr = R_\delta = R_u = 1$. The figure shows the axial force distributions, $F^{\mathrm{as}}(X)$ and $F^{\mathrm{bs}}(X)$, along X direction, and the draw forces at the take-up point, $F^{\mathrm{as}}(X = 1)$ and $F^{\mathrm{bs}}(X = 1)$, vs the draw ratio D_{R}, for different Re.

increase with draw ratio, while the film thickness decreases. The behaviour is monotonic against D_R, except for the force in layer b, which exhibits a weak minimum (see Figure 13). The velocity at the take-up point in layer b follows from Equation (16), which in this case gives $D_R^b = 2D_R - 1$ (see also Figure 11). The film thickness at the take-up point decreases with the draw ratio in both layers (Figure 12), and is equal to $1/D_R$ in layer a, and $1/(2D_R - 1)$ in layer b. The increase in axial forces at the take-up point is further reflected in Figure 13, which depicts the dependence of $F^{as}(X = 1)$ and $F^{bs}(X = 1)$ on D_R for different Reynolds numbers. The figure shows that the draw forces in both layers increases with D_R. When inertia is negligible, the behaviour is essentially logarithmic. The increase becomes essentially linear with D_R in the presence of strong inertia.

4. LINEAR STABILITY ANALYSIS

In this section, linear stability analysis is discussed. The solution procedure for the nonlinear problem is given in detail. The effects of the flow parameters, inertia, viscosity ratio, density ratio and thickness ratio, are examined on the draw resonance for an infinitesimal disturbance.

4.1. The eigenvalue problem

In the stability analysis, gravity effect is neglected because the term with Fr brings extortionate complexity of handling the mathematics in analysis; additionally, for single-layer film casting, the effects of inertia and gravity on linear stability analysis are very similar, both stabilize the process [11], although inertia tends to be the more effective stabilizing force [10]. The stability of the two-layer film casting process is investigated by introducing an infinitesimal one-dimensional disturbance to the field equations. Perturbation variables are introduced in the form

$$\begin{aligned} \Delta^a(X,T) &= \Delta^{as}(X) + \varphi(X)e^{\lambda T} \\ \Delta^b(X,T) &= \Delta^{bs}(X) + \psi(X)e^{\lambda T} \\ U^a(X,T) &= U^{as}(X) + \pi(X)e^{\lambda T} \end{aligned} \tag{25}$$

where $\varphi(X)$, $\psi(X)$ and $\pi(X)$ are complex perturbation amplitudes, λ is a dimensionless growth (or decay) rate of the perturbation variables. Upon substituting for the dependent variables from Equation (25), Equations (13)–(15) become

$$\begin{aligned} &Re[\lambda\pi(\Delta^{as} + R_\rho R_\mu \Delta^{bs}) + (\varphi + \psi R_\rho R_\mu^2)U^{as}U^{as}_{,X} + (\Delta^{as} + R_\rho R_\mu^2 \Delta^{bs}) \\ &\times(\pi U^{as}_{,X} + U^{as}\pi_{,X}) + R_\rho R_\mu(R_u - R_\mu)(\psi U^{as}_{,X} + \Delta^{bs}\pi_{,X})] \\ &\quad = 4[(\varphi_{,X} + \psi_{,X})U^{as}_{,X} + (\varphi + \psi)U^{as}_{,XX} + \pi_{,XX}(\Delta^{as} + \Delta^{bs}) + \pi_{,X}(\Delta^{as}_{,X} + \Delta^{bs}_{,X})] \end{aligned} \tag{26}$$

$$\lambda\varphi + \varphi_{,X}U^{as} + \varphi U^{as}_{,X} + \pi_{,X}\Delta^{as} + \pi\Delta^{as}_{,X} = 0 \tag{27}$$

$$\lambda\psi + R_\mu(\pi_{,X}\Delta^{bs} + \pi\Delta^{bs}_{,X}) + \psi_{,X}(R_u - R_\mu) + R_\mu(U^{as}_{,X}\psi + U^{as}\psi_{,X}) = 0 \tag{28}$$

where all nonlinear terms in the disturbance quantities are neglected because the disturbances are assumed to be infinitesimally small. Since the steady-state solution is not available analytically, then the eigenvalue Equations (26)–(28), and the steady-state Equations (19) and (20) are solved simultaneously.

The differential Equations (26)–(28) lead to an eigenvalue problem, in which the growth (decay) rate parameter λ is complex, $\lambda = \lambda_R + i\lambda_I$. The real part, λ_R, denotes the growth (decay) rate of the disturbance, and the imaginary part, λ_I, is the frequency of draw resonance. For $\lambda_R < 0$, the disturbance decays exponentially with time, and the process is stable. For $\lambda_R > 0$, the disturbance grows exponentially with time, and the process is unstable. Since only the critical conditions for the onset of instability are sought, then one sets neutral stability conditions $\lambda_R = 0$ and $D_R = D_{RC}$ in the analysis. Here, D_{RC} is the critical draw ratio at which the process becomes unstable. For neutral stability, there are eight unknowns, $\lambda_I, \varphi, \psi, \pi$ and D_{RC}, from the eigenvalue problem, in addition to the unknown steady-state velocity, U^{as}. Recall that Δ^{as}, Δ^{bs} and U^{bs} are all given explicitly in terms of U^{as}.

To perform the linear stability analysis, two more equations are needed, in addition to Equations (19), (20), (26)–(28), namely

$$\frac{dD_{RC}}{dX} = 0 \tag{29}$$

$$\frac{d\lambda_I}{dX} = 0 \tag{30}$$

In view of the facts that the critical draw ratio, D_{RC}, and the frequency of draw resonance, λ_I, are constant within the air gap, Equations (29) and (30) are used to complete the system of equations for the stability analysis. By considering the critical draw ratio, D_{RC}, and the frequency of draw resonance, λ_I, to be variables, the eigenvalue problem is now cast as a two-point boundary value problem, upon setting $\lambda_R = 0$. In this case, the relevant boundary conditions at criticality are

$$\begin{aligned} &\varphi(T, X=0) = 0, \quad \psi(T, X=0) = 0, \quad \pi(T, X=0) = 0 \\ &\pi(T, X=1) = 0, \quad U^{as}(X=0) = 1, \quad U^{as}(X=1) = D_{RC} \end{aligned} \tag{31}$$

The solution procedure is now exactly the same as that for the steady-state problem described above.

4.2. Discussion and results

In this section, the linear stability analysis is applied to determine the critical draw ratio for two-layer film casting. The influence of inertia and the properties of the fluid (viscosity ratio and density ratio), as well as the process condition (film thickness ratio), on the critical draw ratio, D_{RC}, and frequency of draw resonance, λ_I, are investigated.

4.2.1. Influence of viscosity ratio. The effect of viscosity on the critical draw ratio, D_{RC}, and frequency of draw resonance, λ_I, is explored by examining the two-layer film casting flow at different viscosity ratios, $R_\mu \in [0.95, 2.0]$. The remaining flow parameters are fixed at $R_\rho = 0.4$, and $R_\delta = R_u = 1.0$. The relationship between the critical draw ratio and viscosity ratio as well as between the frequency and viscosity ratio are depicted in Figure 14 for $Re \in [0, 0.05]$. It is

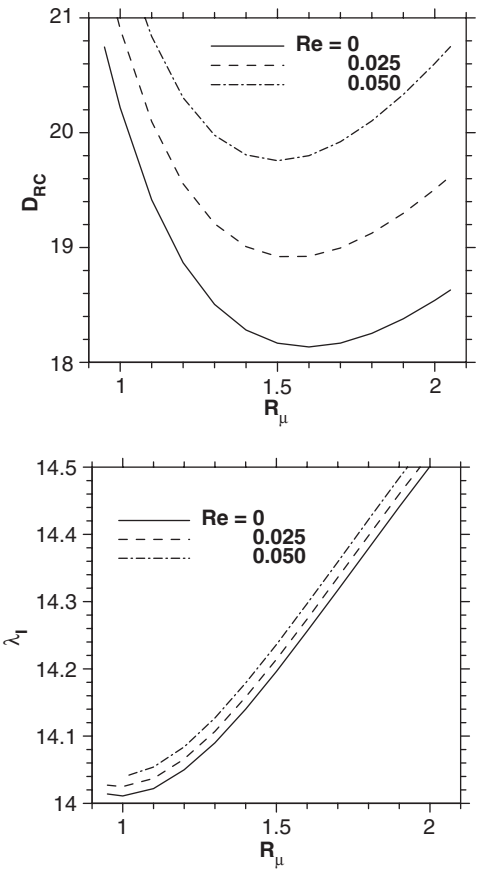

Figure 14. Influence of viscosity ratio on the critical draw ratio and frequency of draw resonance, D_{RC} and λ_1, for $Re \in [0, 0.05]$, $R_\delta = R_u = 1$, $R_\rho = 0.4$.

observed from Figure 14 that viscosity ratio has a significant influence on the critical draw ratio, for any Reynolds number. Typically, the critical draw ratio decreases and reaches a minimum, then increases with R_μ. Thus, flows of fluids with small and large viscosity ratios tend to be relatively stable. There is a non-symmetry with respect to the minimum; the critical draw ratio drops sharply for small R_μ, indicating that the flow is particularly stable at small viscosity ratio. The minimum critical draw ratio occurs in the region $R_\mu \in [1.5, 1.6]$ for any Re. In the absence of inertia, the critical draw ratio for a single-layer film is recovered [1, 10] ($D_{\mathrm{RC}} = 20.2$ for $R_\mu = 1$). It is interesting to note that for R_μ smaller than 1, the two-layer critical draw ratio is always larger than that for single-layer film. Thus, the two-layer film casting process with $R_\mu < 1$ is always more stable than the process of single-layer films. For $R_\mu > 1$, the situation becomes more complicated. In this case, the two-layer film casting process is less stable than that of the single layer only for R_μ slightly larger than one ($1 < R_\mu < 1.6$). In sum, the marginal stability curves in Figure 14 indicate that the stability of the two-layer film casting depends strongly on the layer layout with respect to the take-up rolling process.

The draw resonance frequency corresponding to the onset of instability is also depicted in Figure 14. The curves indicate a monotonic increase of λ_I with viscosity ratio. The increase is generally linear at a rate that is independent of the Reynolds number, but tends to be slow near $R_\mu = 1$. The curves also reflect a linear increase of the frequency with the Reynolds number, for any viscosity ratio. This is in contrast to the more rapid increase of the critical draw ratio with *Re*.

4.2.2. Influence of density ratio. As in the steady-state analysis, the effect of density ratio on the stability is also investigated. In this case, the density ratio, R_ρ, is varied from 0.01 to 1.0. Other parameters of the flow are taken as $R_\mu = 1.5$, and $R_\delta = R_u = 1.0$. The influences of the density ratio on the critical draw ratio and frequency are plotted in Figure 15 for $Re \in [0, 0.05]$. The figure shows, as expected, that the critical draw ratio and frequency are independent of density ratio when inertia is negligible. When the Reynolds number is different from zero, the critical draw ratio and frequency monotonically increase with the density ratio. The neutral stability and frequency curves display essentially a linear increase with R_ρ, at a rate that

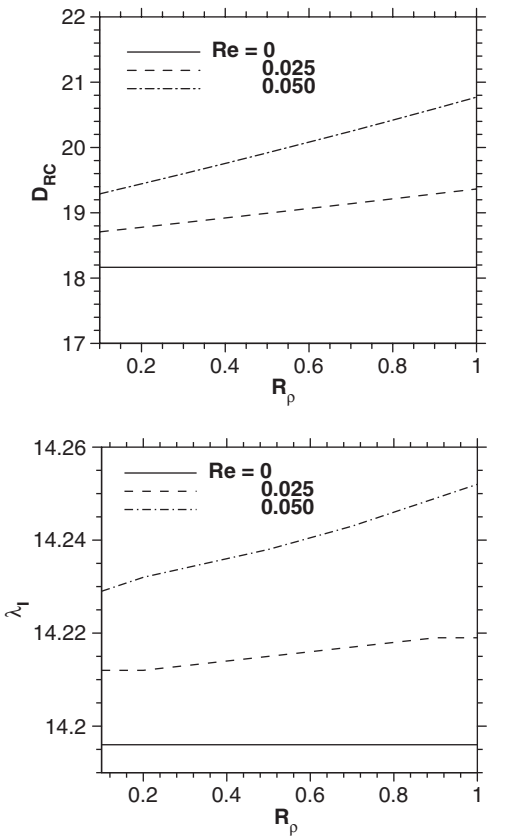

Figure 15. Influence of density ratio on the critical draw ratio and frequency of draw resonance, D_{RC} and λ_I, for $Re \in [0, 0.05]$, $R_\mu = 1.5$, $R_u = R_\delta = 1$.

increases with Re. This result indicates that, in the presence of inertia, increasing fluid density in layer b, or decreasing fluid density in layer a makes the two-layer film casting process more stable. The data in Figure 15 suggest the following dependence of the critical draw ratio and frequency on the Re and R_ρ:

$$D_{\mathrm{RC}} \approx 50ReR_\rho + 18.2, \quad \lambda_{\mathrm{I}} \approx 0.4ReR_\rho + 14.2 \tag{32}$$

These two relations reflect a certain universality of the influence of inertia and density ratio on the stability picture.

4.2.3. Influence of thickness ratio. The influence of thickness ratio on the stability of two-layer film casting is investigated for $R_u = 1$, $R_\rho = 0.4$, $R_\delta \in [0.01, 20]$ and $Re \in [0, 0.05]$, for relatively small and large viscosity ratios. Figures 16 and 17 illustrate the stability picture for $R_\mu = 1.5$ and 0.95, respectively. Recalled from Figure 14 that for $R_\mu > 1 (R_\mu < 1)$, the two-layer film casting is less (more) stable than single-layer film casting. It is shown in Figure 16 ($R_\mu = 1.5$) that the critical draw ratio decreases monotonically with the thickness ratio, but at

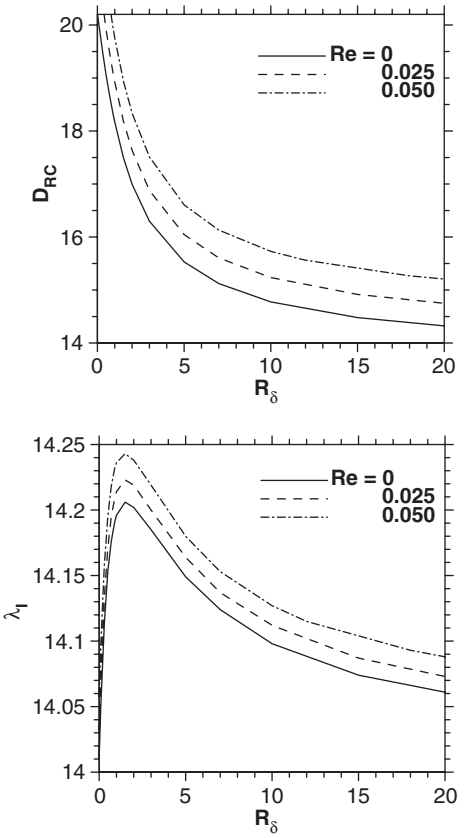

Figure 16. Influence of the thickness ratio on the critical draw ratio and frequency of draw resonance, D_{RC} and λ_{I}, for $Re \in [0, 0.05]$, $R_u = 1$, $R_\mu = 1.5$, $R_\rho = 0.4$.

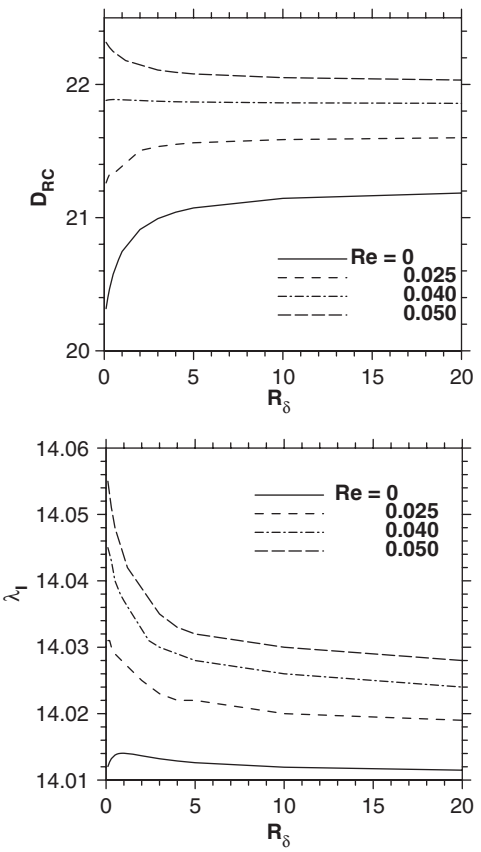

Figure 17. Influence of the thickness ratio on the critical draw ratio and frequency of draw resonance, D_{RC} and λ_{I}, for $Re \in [0, 0.05]$, $R_u = 1$, $R_\mu = 1.5$, $R_\rho = 0.4$.

a rate that varies with R_δ. There is a sharp drop of the critical draw ratio for lower values of R_δ; but the critical draw ratio decreases slowly and tends to level off as R_δ increases further. This result indicates that the process becomes less stable when increasing the thickness of the lower viscosity layer. On the one hand, for the very small R_δ, the thickness of layer a is dominant. In this case, the critical draw ratio is close to that of single-layer film casting. On the other hand, for the large enough R_δ, layer b is the dominantly thick layer, and the neutral stability curve tends to level off and converges to a value smaller than that corresponding to single-layer film. In contrast, the frequency exhibits a maximum that seems to occur at $R_\delta = 1.5$ regardless of the Reynolds number.

The situation in Figure 17 ($R_\mu = 0.95$) is more complicated and inertia is found to have a dramatic effect on the neutral stability curves. Indeed, the critical draw ratio tends to increase (decrease) with R_δ for small (large) Reynolds number. There seems to be a critical Reynolds number (here $Re = 0.04$) at which D_{RC} is not affected by R_δ. For dominantly thick layer a, the critical draw ratio is close to that of single-layer flow. As the thickness of layer b dominates,

the neutral stability curve tends to level off and converge to a value either smaller or larger than that of single-layer flow.

Although the influence of thickness ratio on frequency is overall quantitatively insignificant for both $R_\mu = 1.5$ and 0.95, there are important qualitative differences. For $R_\mu = 0.95$, the frequency does not generally exhibits a maximum, except for creeping flow. The frequency tends to simply decrease with thickness ratio.

4.2.4. Influence of velocity ratio. The effect velocity ratio is investigated by varying R_u from 0.55 to 1.2, while the remaining flow parameters are fixed to $R_\mu = 1.5$, $R_\rho = 0.4$, $R_\delta = 1$ and $Re \in [0, 0.05]$. Figure 18 shows that the critical draw ratio and frequency depend strongly on velocity ratio. It is observed that the influence of velocity ratio is similar to that of viscosity ratio (compare with Figure 14). The minimum critical draw ratio is confined to the range $R_u \in [0.7, 0.8]$ for any Reynolds number. The process appears to be stable for relatively small or large velocity ratio. Steady-state analysis suggests, based on Equation (16), that, for $R_\mu > 1$, the velocity in layer b is larger than that in layer a. This suggests in turn that the flow in layer

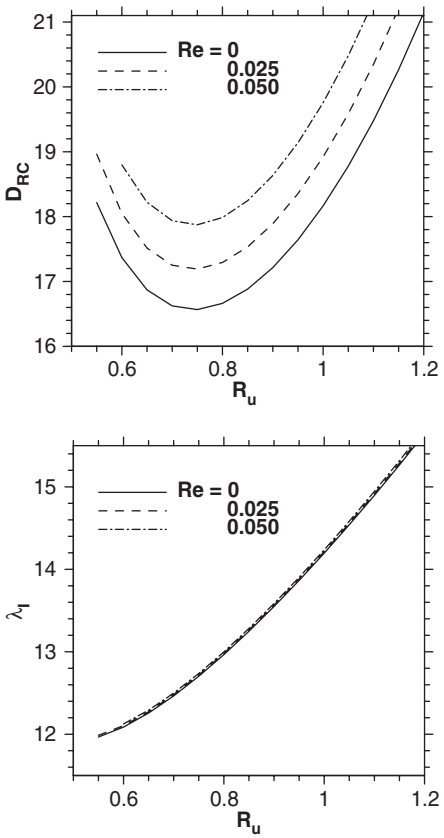

Figure 18. Influence of the velocity ratio on the critical draw ratio and frequency of draw resonance, D_{RC} and λ_1, for $Re \in [0, 0.05]$, $R_\delta = 1$, $R_\mu = 1.5$, $R_\rho = 0.4$.

b plays the dominant role in the destabilization of the process. Moreover, for large velocity ratio ($R_u > 1$), increasing R_u weakens the elongational rate in layer b, therefore leading to a more stable process as Figure 18 suggests. Note that the rate of elongation is reflected by the magnitude of the draw ratio in layer b, which is given from Equation (16) as

$$D_{\mathrm{R}}^{\mathrm{b}} = 1 + \frac{R_\mu (D_{\mathrm{R}} - 1)}{R_u} \tag{33}$$

Simultaneously, for small velocity ratio ($R_u < 0.7$), although Equation (33) shows that decreasing R_u enhances the rate of elongation in layer b, the thickness of layer b decreases, as indicated by Equation (19), thus diminishing the influence of layer b on the stability of the process. This in turn allows further stabilization of the process as shown in Figure 18. The figure indicates that the frequency at the onset of instability increases with R_u almost linearly. It is interesting to observe that although inertia tends to enhance the process stability, it does not seem to have any effect on the frequency as R_u varies.

4.2.5. Influence of inertia. The influence of inertia on the critical draw ratio and frequency is evidently important, based on the results above. This influence, however, may or may not be always significant in practice, depending on flow conditions and parameters. It is also observed that inertia effects need not be strong for inertia to play a determining role. In fact, all flow calculations reported in this study are based on *Re* at most in the order of 10^{-2}, which may very well correspond to practical conditions for film casting. In most polymer film casting operations, the extrude velocity is in the range 0.04–0.1 m/s, the air gap in the range 0.5–0.7 m, the viscosity of the melt is as high as 10^4–10^5 Pa s at the ambient temperature. In this case, the Reynolds number can be small, in the order of 10^{-3}–10^{-4}. However, the viscosity of the fluid is dependent upon temperature and can be given as [12]

$$\mu = \mu_{\mathrm{a}} \mathrm{e}^{-\bar{k}} \tag{34}$$

where μ_{a} is the viscosity at ambient temperature, $\bar{k}$ is the dimensionless viscosity–temperature coefficient, which depends on the difference in temperature of film and ambient temperature. The practical value of $\bar{k}$ [12] is believed to be in the range from 1 to 5. Thus a realistic value for the Reynolds number should be in the order of 10^{-2}.

The results reported in Figures (14)–(18) indicate that inertia has a significant effect on the stability of the two-layer film casting process. The critical draw ratio and the frequency increase essentially linearly with Reynolds number, at a rate that depends on the flow parameters. The Reynolds number has a strong influence on the critical draw ratio; but the frequency of the oscillatory disturbance only exhibits a slight increase with *Re*. The steady-state analysis (see Figure 2) shows that both velocities in layer a and layer b decrease with *Re*. Consequently, the effect of inertia makes the two-layer film casting process more stable. This result is consistent with the predictions of Shah *et al.* [12] on the stability of fibre spinning. They note that the critical draw ratio (20.2) for single-layer film casting is identical to that for Newtonian isothermal spinning [13, 14], if the inertia is negligible. This follows from the fact that, in the case of a two-dimensional disturbance, the two problems are mathematically identical with respect to the perturbation variables. Thus, it is obvious that the influence of inertia on the stability of film casting is consistent with that of fibre spinning.

5. CONCLUSIONS

The steady-state flow and stability of two-layer film casting are investigated in detail in this study. The equations for two-layer flow are derived and solved by taking into account inertia and gravity. The analysis is also applicable to the single-layer flow, for the special case that the flow parameters are the same for the two layers.

Among many variables which may affect the steady-state flow and its stability, the effects of inertia, gravity, viscosity ratio, density ratio and thickness ratio of the fluids as well as the draw ratio are investigated. It is obvious to anticipate that the characteristics of the two-layer flow may fall between those of the single-layer flows of each fluid. In this study, Newtonian fluids are considered. It is not surprising to find that the effects of inertia, gravity and draw ratio on the two-layer steady-state flow and its stability are qualitatively the same with those of single-layer flow [10]. Therefore, only the influences of the parameters related to two-layer character, viscosity ratio, density ratio, velocity ratio and thickness ratio, are addressed here. The viscosity ratio is found to be the only factor among the investigated parameters to alter the relative velocity of the two layers. It is found that if the viscosity ratio is equal to one, the axial velocity is uniform across the two film layers regardless of the value of the other parameters. The film thickness decreases with viscosity ratio, and is independent of density ratio. The axial force in each layer is highly sensitive to these parameters. The draw forces at the take-up point increase with density ratio and viscosity ratio.

The linear stability analysis shows that the critical draw ratio is strongly influenced by the fluid parameters. In general, the stability of the process increases monotonically with density ratio, while it varies non-monotonically with viscosity ratio, velocity ratio and thickness ratio. Similar to the effect on the steady-state flow, the influence of viscosity ratio on the flow stability is significant compared with other parameters. The process stability depends strongly on the layer layout; the two-layer film flow is more stable than a single-layer flow if the viscosity in the layer next to the take-up roll, layer a, is higher than that of the other layer. This result is of practical importance since it illustrates conditions of stability at a high draw ratio for two-layer film casting. The influence of the thickness ratio depends on the viscosity ratio when the layer not in contact with the chill roll, layer b, is dominantly thick. If the thickness of layer a is relatively large, the critical draw ratio tends to that of a single-layer film regardless of the viscosity ratio. In contrast to the effect on the critical draw ratio, the influence of the examined parameters on the frequency is found to be surprisingly insignificant.

Although this study focuses on Newtonian fluids, its procedure and results may serve as a basis for extending the present model to more complicated two-layer film casting systems, for example non-Newtonian fluids. The steady state and the stability analyses should also be applicable to other two-layer flows such as two-phase fibre spinning and two-layer blown film co-extrusion.

REFERENCES

1. Yeow YL. On the stability of extending film: a model for the film casting process. *Journal of Fluids Mechanics* 1974; **66**:613–622.
2. Anturkar NR, Co A. Draw resonance in film casting of viscoelastic fluids: a linear stability analysis. *Journal of Non-Newtonian Fluid Mechanics* 1988; **28**:287–307.
3. Alaie SM, Papanastasiou TC. Film casting of viscoelastic liquid. *Polymer Engineering and Science* 1991; **31**:67–75.

4. Park C-W. A study on bicomponent two-layer slot cast coextrusion. *Polymer Engineering and Science* 1991; **31**:197–203.
5. Pis-Lopez ME, Co A. Multilayer film casting of modified Giesekus fluids. Part 1. Steady-state analysis. *Journal of Non-Newtonian Fluid Mechanics* 1996; **66**:71–93.
6. Pis-Lopez ME, Co A. Multilayer film casting of modified Giesekus fluids. Part 2. Linear stability analysis. *Journal of Non-Newtonian Fluid Mechanics* 1996; **66**:95–114.
7. Middleman S. *Fundamentals of Polymer Processing*. McGraw-Hill: New York, 1977; 509.
8. Agassant J-F, Avenas P, Sergent J-Ph, Carreau PJ. *Polymer Processing Principles and Modeling*. Hanser Publishers: Berlin, 1991.
9. Kumar, Gupta RK. *Fundamentals of Polymer Engineering* (2nd edn). Marcel Dekker: New York, 2003; 674.
10. Cao F. *M.E.Sc. Thesis*, The University of Weastern Ontario, London, Ontario, Canada, 2003.
11. Doufas A, McHugh A, Miller C. Simulation of melt spinning including flow-induced crystallization. Part I. Model development and predictions. *Journal of Non-Newtonian Fluid Mechanics* 2000; **92**:27–66.
12. Shah YT, Pearson JRA. On the stability of nonisothermal fiber spinning—general case. *Industrial and Engineering Chemistry Fundamentals* 1972; **11**:150–153.
13. Fisher RJ, Denn MM. Finite-amplitude stability and draw resonance in isothermal melt spinning. *Chemical Engineering Science* 1975; **30**:1129–1134.
14. Pearson JRA, Matovich MA. Spinning a molten threadline: stability. *Industrial and Engineering Chemistry Fundamentals* 1969; **8**(4):605–609.

